

Bulk and Solution Copolymerization of Methyl Methacrylate and Vinyl Acetate

M. J. SCORAH, H. HUA, M. A. DUBÉ

Department of Chemical Engineering, University of Ottawa, Ottawa, Ontario K1N 6N5, Canada

Received 19 July 2000; accepted 4 December 2000

ABSTRACT: A series of batch, bulk and solution (in toluene) copolymerizations of methyl methacrylate and vinyl acetate was performed under various reaction conditions to high monomer conversions. In addition, low conversion bulk experiments were performed to estimate monomer reactivity ratios using the error in variables model method, based on terminal model (Mayo–Lewis) kinetics. A combination of the low and high conversion data with data from a previous study yielded reactivity ratio (r) estimates of 27.465 and 0.0102 for r_{MMA} and r_{VAc} , respectively, using the integrated copolymer composition (Meyer–Lowry) equation. In the high conversion experiments the effects of various factors on the reaction rate, cumulative copolymer composition, number- and weight-average molecular weights, and molecular weight distribution were studied. The factors included the monomer feed composition, initiator concentration, temperature, solvent concentration, and the addition of *n*-dodecyl mercaptan chain transfer agent. These factors were examined in light of the wide difference in the monomer reactivity ratios. © 2001 John Wiley & Sons, Inc. *J Appl Polym Sci* 82: 1238–1255, 2001

Key words: methyl methacrylate; vinyl acetate; reactivity ratios; copolymerization; toluene; bulk; solution

INTRODUCTION

Product quality control in copolymerizations is often quite challenging. The final product properties are a function of the polymer composition and are thus dependent on the reactivity ratios (r), which are defined by the ratios of the homopropagation and cross-propagation rate constants as follows:

$$r_1 = \frac{k_{p11}}{k_{p12}}$$

$$r_2 = \frac{k_{p22}}{k_{p21}} \quad (1)$$

where $k_{p_{ij}}$ is the rate constant for the addition of monomer j to a radical chain on which the active radical center is located on a monomer i unit. The reactivity ratios are parameters in the Mayo–Lewis equation, which is also referred to as the terminal model for propagation¹:

$$\frac{F_1}{F_2} = \frac{(r_1 f_1 + f_2) f_1}{(f_1 + r_2 f_2) f_2} \quad (2)$$

where F_1 and F_2 are the overall instantaneous mole fractions of monomer 1 and monomer 2 in the copolymer, respectively; and f_i is the mole fraction of monomer i in the reaction mixture. These reactivity ratios are not only vital to the

Correspondence to: M. A. Dubé.
Contract grant sponsor: Natural Sciences and Engineering Research Council (NSERC) of Canada.

Journal of Applied Polymer Science, Vol. 82, 1238–1255 (2001)
© 2001 John Wiley & Sons, Inc.

prediction of polymer composition but are also essential to the prediction of microstructure, polymerization rate, and molecular weight distribution. These in turn directly influence the final properties of the copolymer.

A particularly challenging situation develops when the reactivity ratios of the copolymer differ greatly from one another. For example, the reactivity ratios for copolymer systems that include vinyl acetate (VAc) with acrylic monomers tend to be prone to this. The reactivity ratios for the butyl acrylate/VAc (BA/VAc) and methyl methacrylate/VAc (MMA/VAc) systems are reported to be $r_{BA} = 5.939$ and $r_{VAc} = 0.0262$ for BA/VAc and $r_{MMA} = 24.025$ and $r_{VAc} = 0.0261$ for MMA/VAc.² Similar values are reported for methyl acrylate/VAc,^{3,4} butyl methacrylate/VAc,⁵ and ethyl methacrylate/VAc.⁶ For all of these systems, these differing reactivity ratios imply that the acrylic monomer is preferred for addition to the growing copolymer chain over the VAc monomer. As a result, if operating under batch reaction conditions, a drift in the copolymer composition occurs. In view of the final properties of the copolymer, the resulting broad composition distribution is unacceptable. Thus, semibatch feed policies are often employed to control the copolymer composition.^{7,8} These feed policies depend on the accuracy of the reactivity ratios. To that end, highly reliable and accurate statistical techniques are needed to estimate reactivity ratios. The method shown to be the most reliable based on these criteria is that employing the error in variables model (EVM).^{9–12} Thus, we are interested in gaining a better understanding of one copolymer system, MMA/VAc, which poses these challenges.

To begin, we require accurate reactivity ratio estimates. In addition, kinetic knowledge from batch experiments would be useful in uncovering potential misunderstandings about the reaction mechanism or in identifying model parameters requiring improved estimates. Because of the wide difference in reactivity ratios and the proximity of the value for r_{VAc} to zero, numerical difficulties make the calculation of the reactivity ratios for the MMA/VAc system rather challenging. Several studies were published that dealt with these estimations.^{2,13–18} Studies of the batch copolymerization of MMA/VAc largely focused on the estimation of the termination and propagation rate parameters.^{13,18–21} The study by Ma et al.¹⁸ examined the propagation and termination reactions at 40°C by using the rotating-sector technique. They showed that the composition curve for this particular system agreed with the

terminal model and with the findings of Brar and Charan.²² Ma et al.¹⁸ observed only a moderate penultimate unit effect for the copolymerization rate for the MMA/VAc system.

The studies mentioned above deal only with the estimation of reactivity ratios or rate parameters. There are few published data of the *bulk* copolymerization of MMA and VAc with the exception of the experiment by Dubé and Penlidis² in which the copolymer composition and molecular weight were measured to high conversion levels and the experiment by Busfield and Low.¹⁵ In the case of solution copolymerization of MMA and VAc, Busfield and Low¹⁵ discussed the effects of five different solvents on the rate of copolymerization of MMA/VAc in experiments limited to low conversions. A detailed study presented by Choi and Butala²³ researched open loop control strategies for the semibatch solution (in toluene) copolymerization of MMA and VAc. They reported data for the composition and molecular weight for these experiments and also conducted a batch experiment. A larger body of work on the MMA/VAc copolymerization is reported for emulsion polymerization.^{24–26}

This article continues and expands upon the work completed on the MMA/VAc system by Dubé and Penlidis.² Several high conversion bulk and solution experiments were carried out in which conversion, cumulative copolymer composition, and cumulative number- and weight-average molecular weights were measured. The reaction conditions were varied in each experiment in order to study the effects of temperature, feed composition, initiator concentration, solvent concentration, and the addition of a chain transfer agent (CTA). Dubé and Penlidis² identified a two-stage rate effect that occurred during the bulk copolymerization of MMA and VAc. This work investigates in more detail the occurrence of this effect and how it is influenced by varying the reaction conditions. The improved reactivity ratio estimates were also determined for the MMA/VAc system using appropriate experimental design and statistical data analysis techniques.

EXPERIMENTAL

Reagent Purification

The purification of reagents was performed according to classical methods.^{27,28} The initiator 2,2'-azo-bisobutyronitrile (Polysciences Inc.)

Table I Full Conversion Experiment Conditions

Experiment	Temperature (°C)	$f_{1,0}$	Initiator Concn (mol/L)	CTA Concn (mol/L)
1	60	0.20	0.1	0
2	60	0.40	0.1	0
3 (replicate)	60	0.40	0.1	0
4	60	0.50	0.1	0.0058
5 (replicate)	60	0.50	0.1	0.0058
6	60	0.75	0.1	0.0058
7	70	0.20	0.1	0.0058
8	70	0.40	0.1	0.0058
9 (50 wt % toluene)	60	0.40	0.05	0.05
10 (50 wt % toluene)	60	0.50	0.05	0.025
11 (50 wt % toluene)	60	0.40	0.1	0.025
12 (50 wt % toluene)	60	0.50	0.1	0.025

was recrystallized 3 times from absolute methanol. The monomer MMA (Aldrich Chemical Co.) was washed 3 times with a 10% sodium hydroxide solution, washed 3 times with distilled deionized water, dried over calcium chloride, freshly distilled at 25°C under a vacuum for at most 24 h before use, and stored at -10°C. The VAc monomer (Aldrich) was freshly distilled at 20°C under a vacuum for at most 24 h before use and stored at -10°C. In some of the high conversion experiments a CTA, *n*-dodecyl mercaptan, was used in order to observe its effect on the molecular weight. The CTA and each solvent used over the course of the experiments and in the characterization of the copolymers [toluene, ethanol, acetone, tetrahydrofuran (THF), and chloroform-*d*] were used as packaged.

Reactivity Ratio Estimation Experiments

The design of the reactivity ratio experiments followed the criteria developed by Tidwell and Mortimer.²⁹ They proposed a basis for selecting the experimental conditions while taking into account the sensitivity of the reactivity ratio estimates to the errors in determining the copolymer composition. Their design recommended completing several replicate runs at two different monomer feed compositions. The initial feed compositions for monomer 1 are given by the following equations:

$$f'_{1,0} = 2/(2 + r_1) \quad (3)$$

$$f''_{1,0} = r_2/(2 + r_2) \quad (4)$$

Throughout this article, monomer 1 refers to MMA while monomer 2 corresponds to VAc.

In order to calculate the required monomer feed compositions, initial estimates of the reactivity ratios are needed. At a temperature of 60°C, Dubé and Penlidis² obtained values of $r_1 = 26.200$ and $r_2 = 0.0153$. Substituting these initial estimates into eqs. (3) and (4), $f'_{1,0}$ and $f''_{1,0}$ were determined to be 0.07093 and 0.007572, respectively. Because of the large difference between the reactivity ratios for MMA/VAc, copolymer composition drift becomes significant at very low conversions.² Thus, in order to minimize composition drift, conversions of 1.5 wt % were not exceeded.

The experiments were conducted in glass ampoules (~15-mL capacity). The monomers and initiator were weighed, combined, and then pipetted into the ampoules. Four replicate ampoules were created for each feed composition. The ampoules were degassed by several vacuum-freeze-thaw cycles, sealed, and placed in a 60°C water bath for a recorded time period. The ampoules were then

Table II Experimental Results for Reactivity Ratio Estimation at 60°C and with 0.5M [AIBN]

$f_{1,0}$	Conversion (wt %)	\bar{F}_1
0.00758	0.856	0.372
0.00758	1.072	0.349
0.00758	0.906	0.312
0.00758	1.008	0.305
0.0709	1.284	0.760
0.0709	1.308	0.755
0.0709	1.280	0.776
0.0709	1.396	0.758

Table III Reactivity Ratio Estimates Using Mayo-Lewis Equation

Source of Data	r_1	r_2
Present study	35.383	0.0118
Dubé and Penlidis ²	24.025	0.0261
Dubé and Penlidis ² and present study	22.760	0.0147

immediately cooled, weighed, scored, broken, and the contents were poured into a 10-fold excess of ethanol. The empty ampoules were then reweighed. The copolymer was precipitated in the ethanol and then dried in a vacuum oven (40°C) until a constant weight was reached.

The conversion was based on the total polymer and determined by means of gravimetry. The polymer product was analyzed for cumulative polymer composition by proton NMR (¹H-NMR) spectrometry.

High Conversion Experiments

The design of the high conversion experiments was complementary to the work completed by Dubé and Penlidis² for bulk MMA/VAc copolymerization. Thus, experiments were chosen at similar temperatures and at feed compositions other than 30 mol % MMA. The experimental conditions are shown in Table I. The experimental factors that were varied included the temperature, monomer feed composition ($f_{1,0}$), initiator concentration, CTA concentration, and solvent concentration. Some replicate runs were also performed.

High conversion experiments were carried out in glass ampoules with an 18-cm length, 0.8-cm outer diameter, and ~4-mL capacity. This size was chosen to minimize potential nonisothermal effects.^{30,31} Monomer feed solutions were prepared by combining weighed amounts of the monomers and initiator in a flask. Toluene solvent was added for experiments 9–12. For experiments 4–12 a measured amount of CTA was pipetted into the flask. Each monomer feed was pipetted into several numbered ampoules, which was typically 10 ampoules per experiment. The ampoules were then treated exactly as in the reactivity ratio experiments. Some of the high conversion samples were in a glassy state, preventing the easy removal of the entire sample from the ampoule. In these cases the mixture was frozen in

liquid nitrogen and the ampoule broken. A piece of the frozen monomer-polymer mixture was weighed and then left to dissolve in toluene at -5°C. The polymer was precipitated in a 10-fold excess of ethanol and dried to a constant weight similar to the other samples.

The conversion based on the total polymer was determined by gravimetry. The polymer product was analyzed for cumulative polymer composition by ¹H-NMR spectrometry. Selected samples were analyzed for cumulative number- and weight-average molecular weight by gel permeation chromatography (GPC).

Characterization

A Bruker AMX 500 NMR spectrometer was used for the polymer composition analysis.³² The analysis was completed in deuterated chloroform at room temperature. The relative amounts of MMA and VAc bound in the copolymer were then estimated from the areas under the absorption peaks of the spectra. The spectral peak for the three protons in the -OCH₃ group in MMA was at $\delta = 3.6$ ppm and that for the α -hydrogen in VAc was at $\delta = 4.9$ ppm.

The cumulative number- and weight-average molecular weights were determined with a Waters Associates GPC chromatograph equipped with a Waters 410 refractive index detector. Three Waters Ultrastayragel packed columns (10³, 10⁴, and 10⁶ Å) were installed in series. The THF (HPLC grade, EM Science) was filtered and used as the eluent at a flow rate of 0.3 mL/min at 38°C. The calibration of the instrument was performed using polystyrene standards. The standards and samples were prepared in THF (0.2% (w/v) solutions) and filtered prior to injection through 0.45- μ m filters to remove high molecular weight

Table IV Literature Values of Reactivity Ratios for MMA/VAc

Source	r_1	r_2	Conditions
Atherton and North ¹³	28.6	0.035	30°C, bulk
Bevington and Johnson ¹⁴	26	0.030	60°C, solution
Busfield and Low ¹⁵	24	0.029	49°C, bulk
Kuo and Chen ¹⁶	21.2	0.016	60°C, bulk
Bauduin et al. ¹⁷	29.9	0.0445	60°C, bulk
Ma et al. ¹⁸	27.8	0.014	40°C, bulk
Dubé and Penlidis ²	26.200	0.0153	60°C, bulk

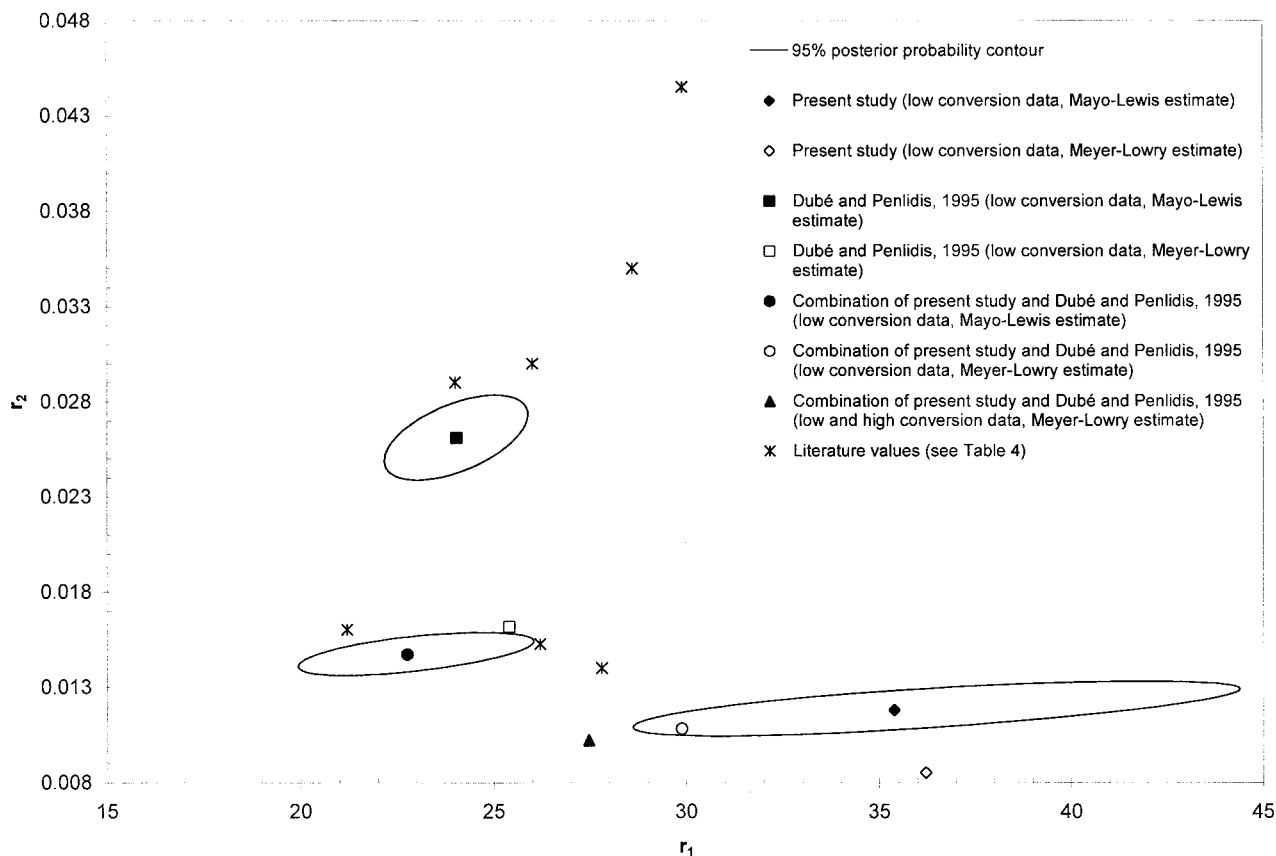


Figure 1 The 95% posterior probability contours and point estimates of the reactivity ratios.

gel, if present. Millennium 32™ software (Waters) was used for data acquisition and manipulation.

The determination of the absolute cumulative number- and weight average molecular weights was accomplished using a universal calibration curve. This curve was constructed using the Mark–Houwink, K , and α parameters determined in THF. The constants for pMMA were $K = 0.0128$ mL/g and $\alpha = 0.690$, for pVAc were $K = 0.0156$ mL/g and $\alpha = 0.708$, and for polystyrene

were $K = 16$ mL/g and $\alpha = 0.700$.^{33,34} The K and α values for the copolymers were obtained using weighted averages based on the cumulative copolymer composition data.

RESULTS

Reactivity Ratio Estimation

Table II lists the monomer feed compositions, final conversion, and copolymer composition (\bar{F}_1)

Table V Reactivity Ratio Estimates Using Meyer–Lowry Equation

Source of Data	r_1	r_2
Present study reactivity ratio data	36.205	0.0085
Dubé and Penlidis ² reactivity ratio data	25.395	0.0162
Low conversion reactivity ratio data from Dubé and Penlidis ² and present study	29.881	0.0108
All bulk (low and high conversion) data from Dubé and Penlidis ² and present study	27.465	0.0102

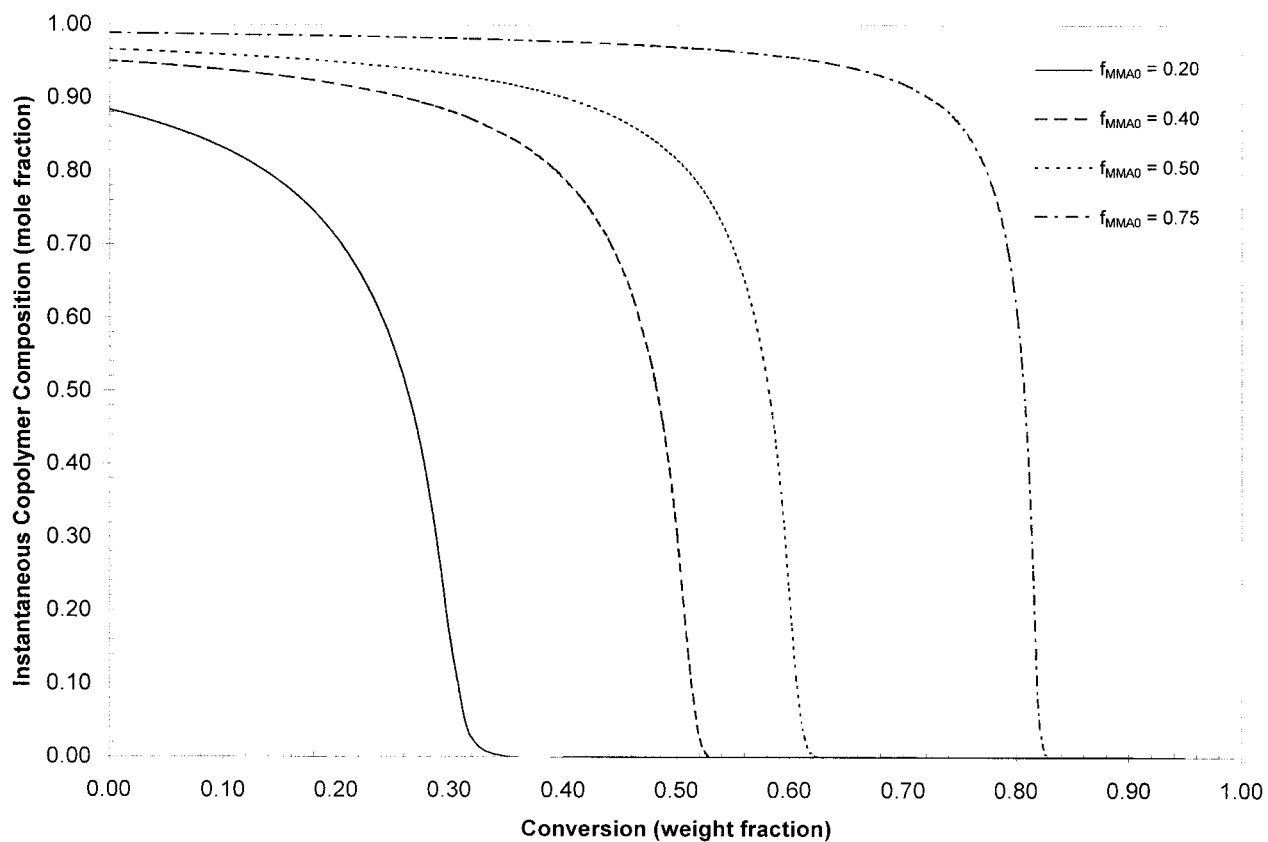


Figure 2 The instantaneous copolymer composition versus the conversion.

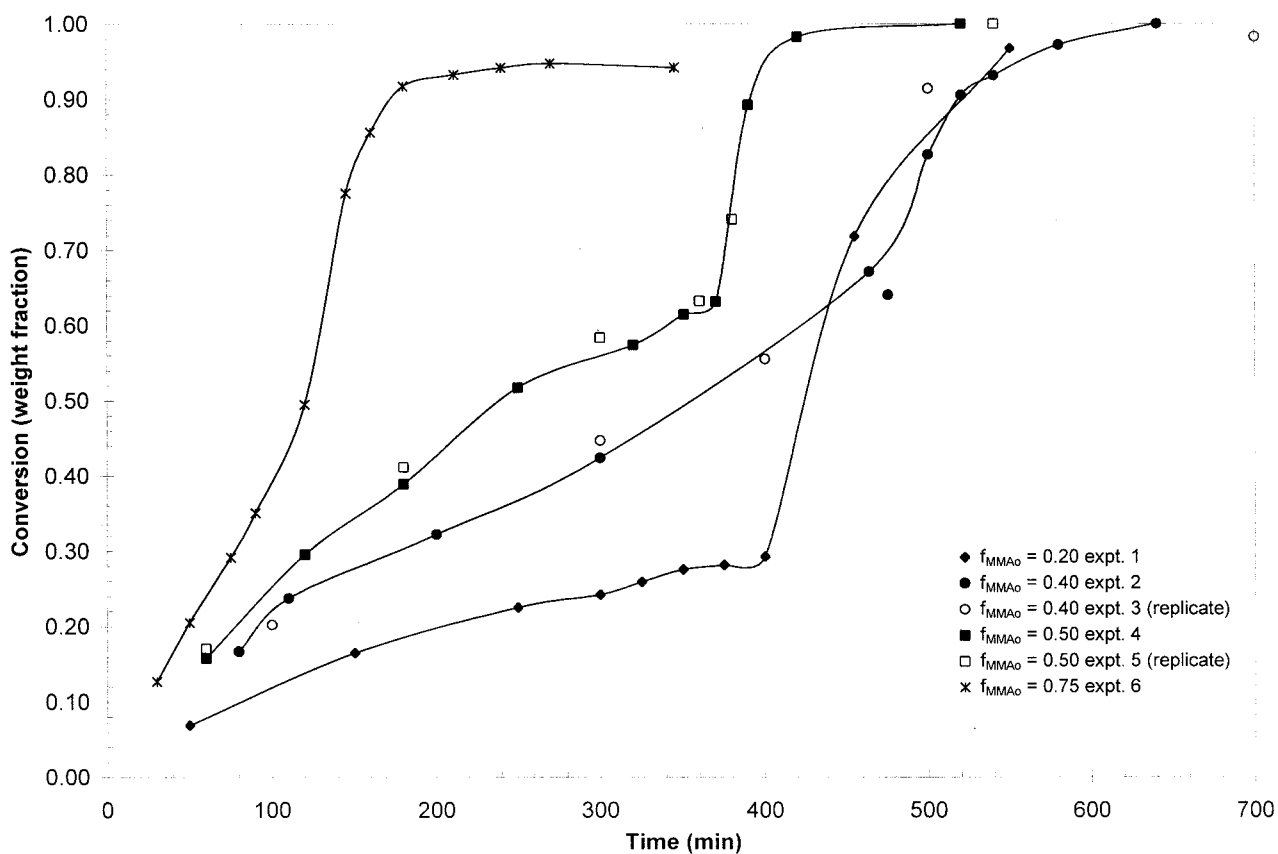


Figure 3 The conversion versus the time at 60°C for bulk copolymerizations.

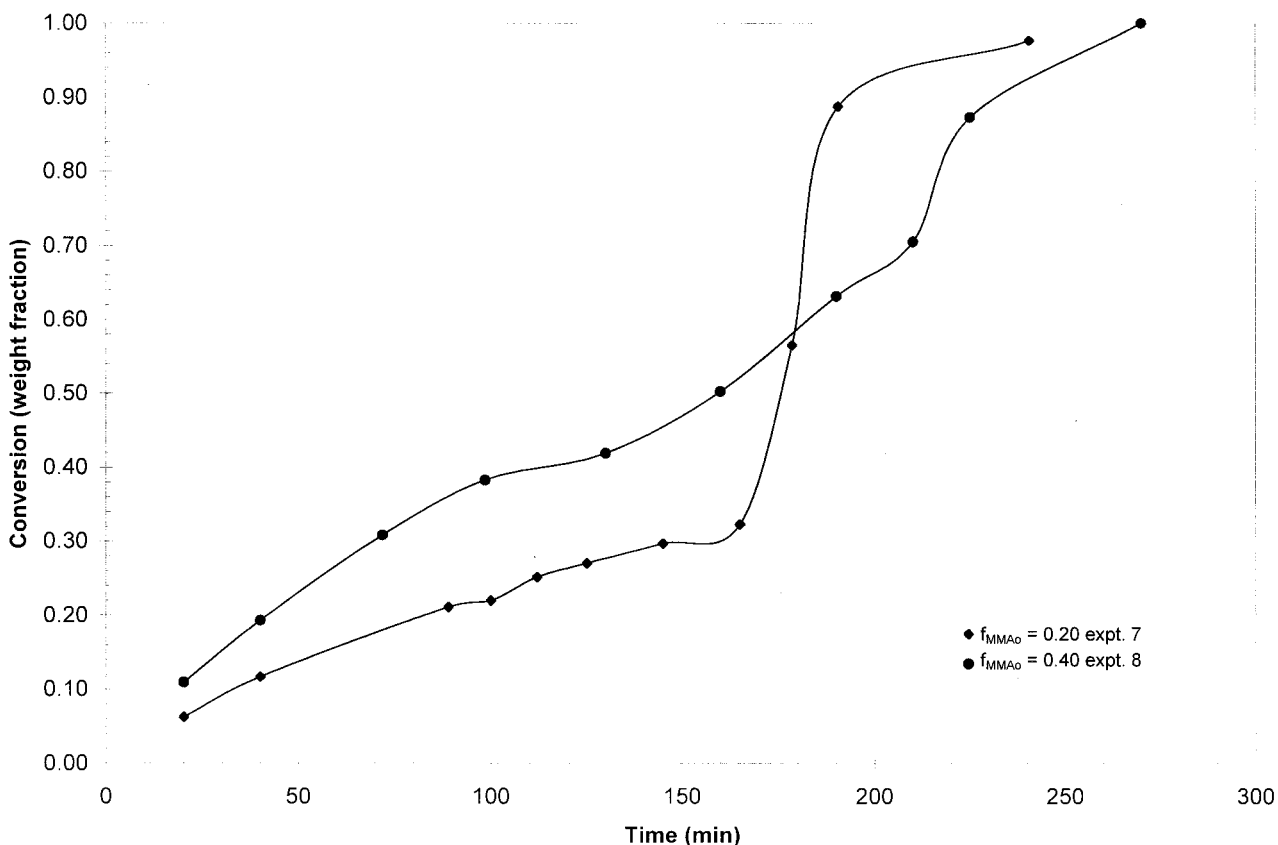


Figure 4 The conversion versus the time at 70°C for bulk copolymerizations.

for the eight reactivity ratio estimation experiments, which were four replicate runs completed at two different monomer feeds. Low conversion levels (<1.4 wt %) were maintained for each experiment, and thus the copolymer composition drift was minimized.

The data were analyzed through the use of two different methods. In the first case, the analysis was performed by employing a computer program known as RREVM.¹⁰⁻¹² RREVM solves the well-known Mayo-Lewis equation or terminal model¹ [see eq. (2)]. The RREVM program relies on the EVM and therefore takes into account the error in the dependent (i.e., copolymer composition) and independent (i.e., monomer feed composition) variables.

In a second analysis, the reactivity ratio estimation was performed using a computer program based on the Meyer-Lowry integrated copolymer composition equation³⁵:

$$x = 1 - \left(\frac{f_1}{f_{1,0}} \right)^\alpha \left(\frac{1 - f_1}{1 - f_{1,0}} \right)^\beta \left(\frac{f_{1,0} - \delta}{f_1 - \delta} \right)^\gamma \quad (5)$$

where x is the monomer conversion and $f_{1,0}$ is the initial mole fraction of monomer 1 and

$$\alpha = \frac{r_2}{1 - r_2} \quad (6)$$

$$\beta = \frac{r_1}{1 - r_1} \quad (7)$$

$$\gamma = \frac{1 - r_1 r_2}{(1 - r_1)(1 - r_2)} \quad (8)$$

$$\delta = \frac{1 - r_2}{2 - r_1 - r_2} \quad (9)$$

This second method was performed to ensure that the use of the Mayo-Lewis equation was valid. Any significant differences between the two sets of results would indicate that the composition drift in the samples was too large to be ignored and that the integrated form (Meyer-Lowry) rather than the differential form (Mayo-Lewis) of the composition equation should be employed.

Reactivity ratio estimates obtained using RREVM (based on the Mayo-Lewis equation) are shown in Table III. The results from Dubé and Penlidis,² as well as a combination of their data

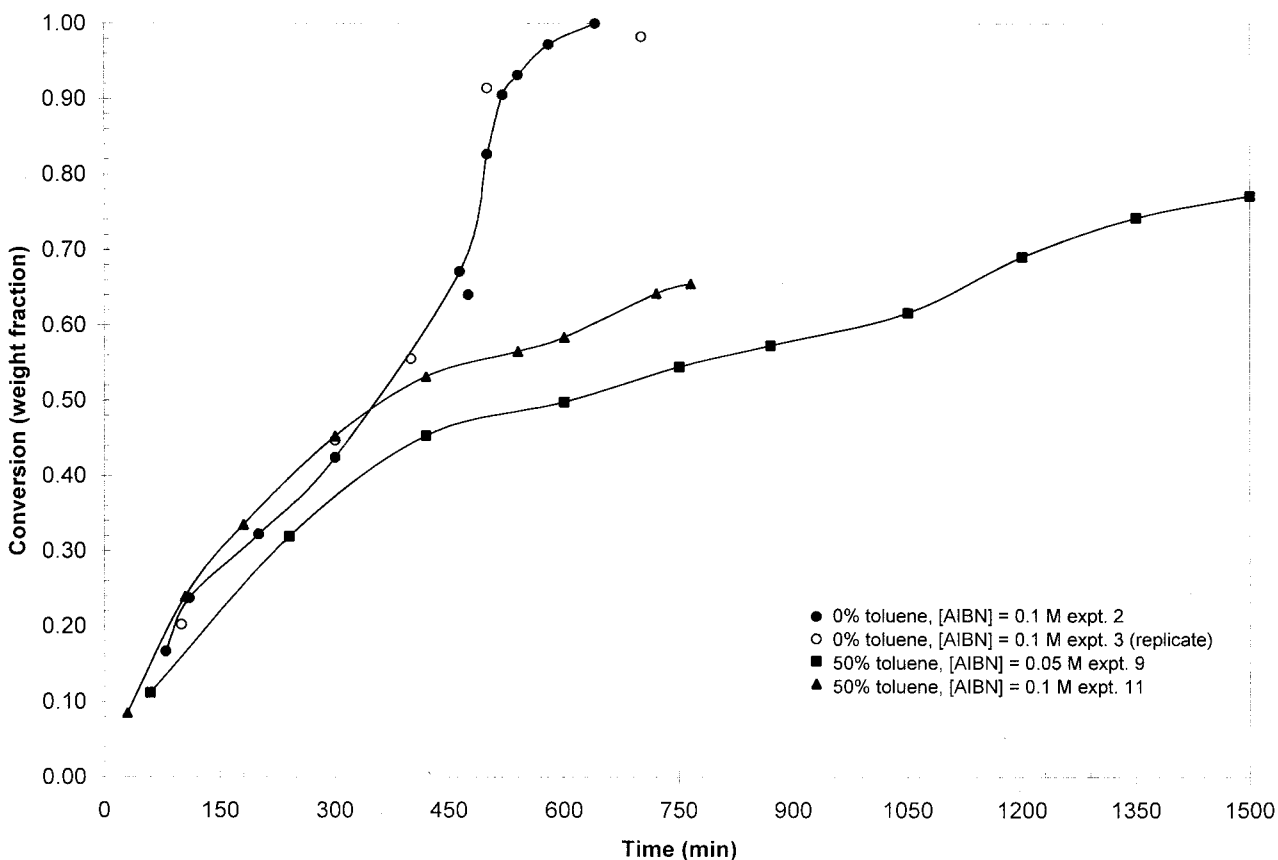


Figure 5 The conversion versus the time at 60°C ($f_{1,0} = 0.40$) in bulk versus solution polymerizations.

with ours, are also shown. Reactivity ratios from other literature sources are shown in Table IV. Figure 1 provides the literature values from Table IV and the 95% posterior probability contour plots for the three sets of reactivity ratio estimates given in Table III. The 95% posterior probability contours revealed the uncertainty in the reactivity ratios. This was more appropriate than using confidence intervals because of the high degree of correlation between the two reactivity ratios.

Figure 1 displays the evident scatter in the data. There are two reasons for the discrepancy of the reactivity ratios estimated from the low conversion data in this work. The first is that the Tidwell–Mortimer²⁹ experimental design is an iterative one, and the present study can be considered as the third iteration in a series. Data from Busfield and Low¹⁵ (iteration 1) were used to generate the experimental conditions in Dubé and Penlidis² (iteration 2), and then their results² were used to generate the monomer feed compositions for the present study (iteration 3). This iterative process yielded a similar scatter in the

results for the BA/MMA system.³⁶ A second possible explanation for the differing reactivity ratios is the extremely low value of r_2 (or r_{VAc}) relative to r_1 (or r_{MMA}). Such low values are likely to cause numerical difficulties and magnify experimental errors during parameter estimation. Nonetheless, improved estimates were obtained when the data from Dubé and Penlidis² were combined with that of this study. These estimates were quite similar to several of the literature values, specifically those of Kuo and Chen.¹⁶ From Figure 1 and Table IV it is apparent that these estimates fall within a window of values. In any case, these estimates from the low conversion data are considered to be limited. The use of high conversion data would necessarily improve these estimates, as discussed below.

Table V lists the reactivity ratios resulting from the parameter estimation based on the Meyer–Lowry equation. The first three rows contain the reactivity ratio estimates calculated from the low conversion data used for the Mayo–Lewis analysis, which was based on the Tidwell–Mor-

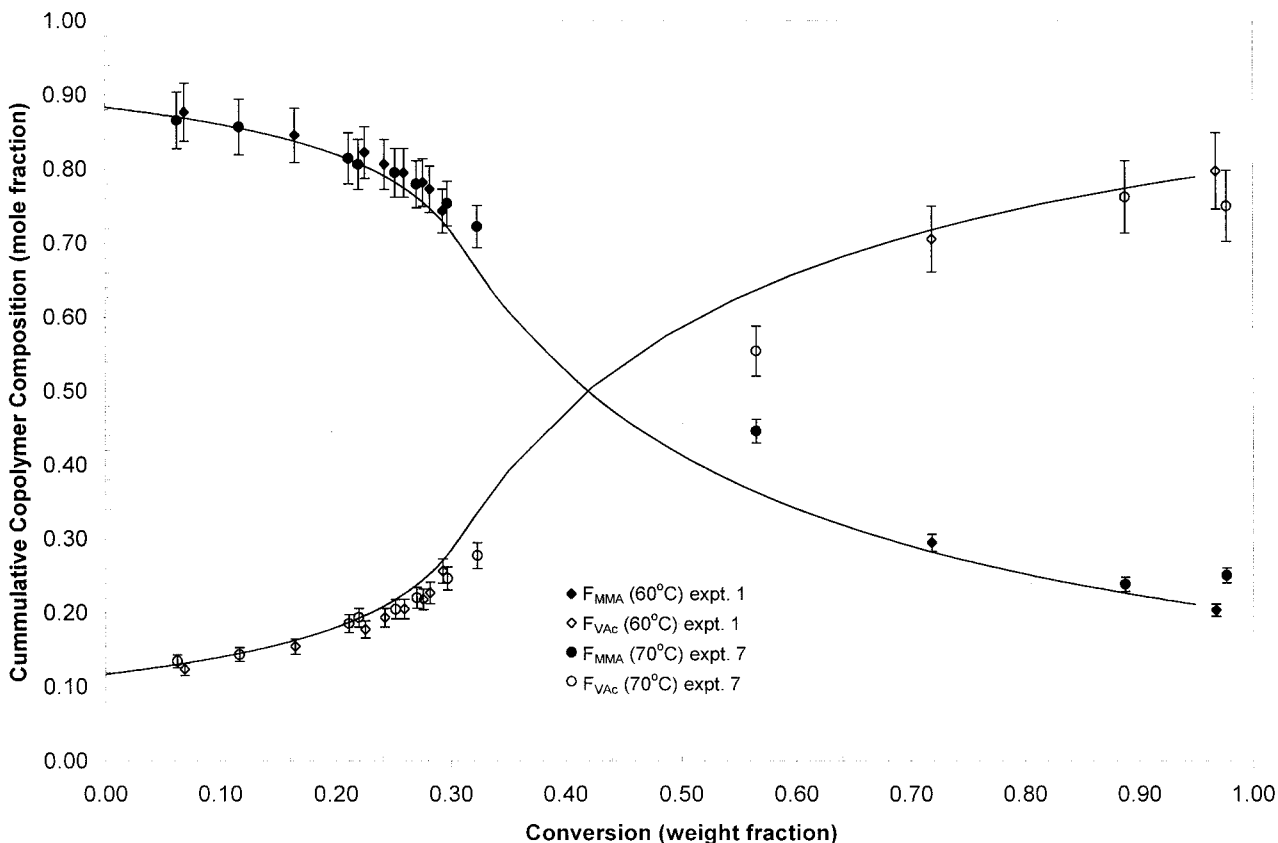


Figure 6 The cumulative copolymer composition versus the conversion ($f_{1,0} = 0.20$).

timer criterion. These estimates are also shown in Figure 1. When comparing these estimates to their corresponding values in Table III, a difference can be seen. This suggests that the composition drift may not have been a negligible factor. Dubé and Penlidis² showed that MMA/VAc copolymers exhibited severe composition drift even at very low conversions and our results confirmed this. The last set of reactivity ratio estimates in Table V was calculated by combining all low and high conversion bulk data from Dubé and Penlidis² with the data from this study for a total of 87 data points. Because of the possibility of solvent effects on the reactivity ratios,¹⁵ data from the solution polymerizations were not included in the parameter estimations. These estimates, $r_1 = 27.465$ and $r_2 = 0.0102$, compared favorably with the literature values in Table IV (see also Fig. 1).

A further, important observation is that the estimates for r_1 are considerably larger than that for r_2 . Reactivity ratio estimates are ratios of the propagation rate constants and provide an indication of how the MMA/VAc system be-

haves. Because r_1 is much larger than one, it indicates that radical chains ending in MMA prefer to add MMA monomer as opposed to VAc monomer [see eq. (1)]. Furthermore, because r_2 is much smaller than one, it implies that radical chains ending in VAc also prefer to add MMA rather than VAc [see eq. (1)]. The effect of a system having two significantly different reactivity ratios can be seen in Figure 2 where model predictions of the instantaneous copolymer composition are plotted versus the conversion using our reactivity ratio estimates $r_1 = 27.465$ and $r_2 = 0.0102$. The graph shows the instantaneous mole fraction of MMA bound in the copolymer for the feed conditions used in this study. In each case, the predictions indicate that at low conversions the copolymer formed is mostly composed of MMA. Near the point where the MMA monomer is completely consumed, a sharp decrease in the amount of MMA bound in the copolymer is manifested. As higher conversions are reached, the polymer being formed is essentially VAc homopolymer.

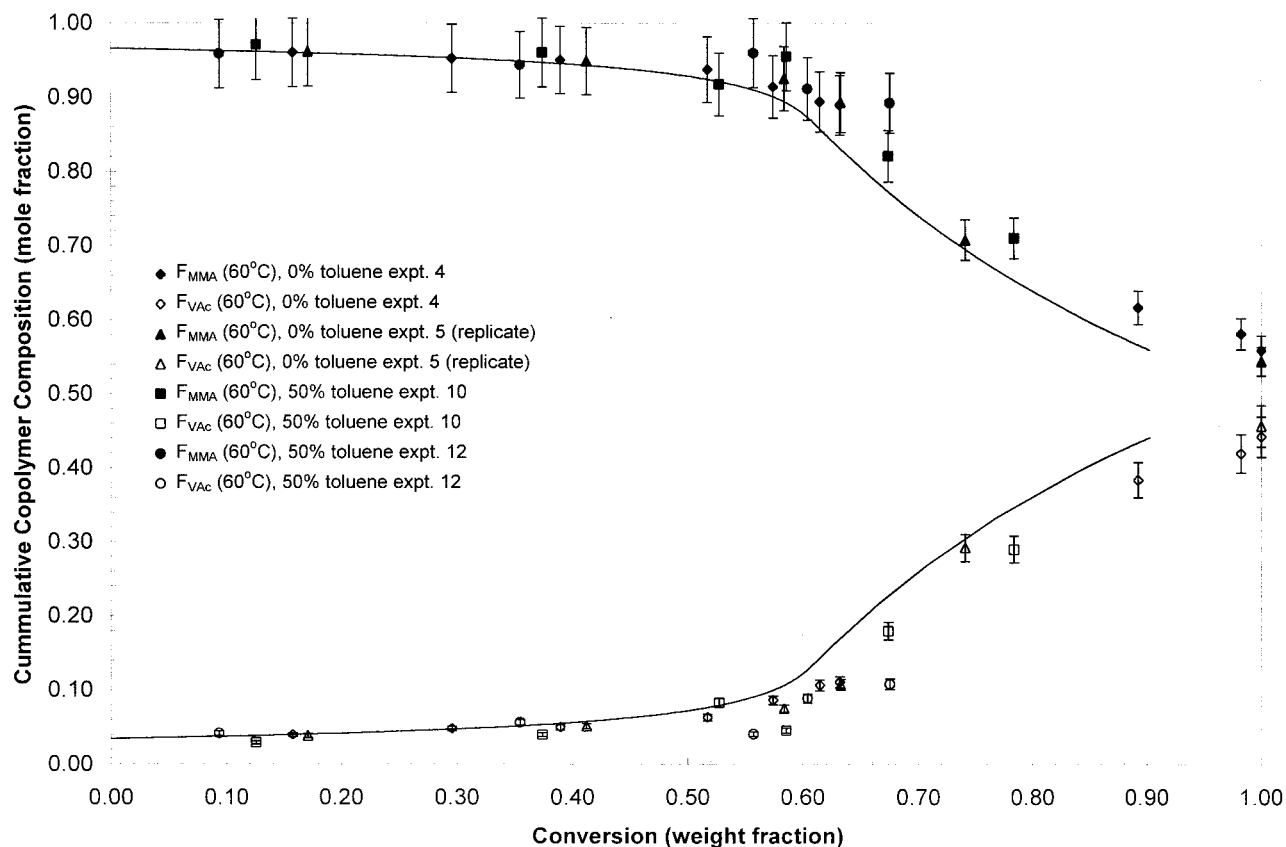


Figure 7 The cumulative copolymer composition versus the conversion ($f_{1,0} = 0.50$).

High Conversion Experiments

Conversion

Plots of conversion versus time are presented in Figures 3–5. The solid lines in the figures are fitted curves and not model predictions. Figure 3 provides a comparison of the experiments completed at 60°C in bulk (experiments 1–6, Table I). It was observed that increases in the amount of MMA in the feed resulted in higher initial reaction rates. The data also exhibited a two-stage rate effect.² During the first part of the reaction, the rate of polymerization followed a trajectory typical of solution polymerizations. This initial “solutionlike” regime was followed by an abrupt increase in conversion. At high conversion levels ($x > 0.90$), the polymerization slowed to a limiting conversion level. This two-stage rate effect was due to the large difference between the reactivity ratios ($r_1 = 27.465$ and $r_2 = 0.0102$, Table V). These values indicated that radical chains ending in either MMA or VAc preferred to add a MMA monomer unit. Thus, MMA dominated the first part of the polymerization until it was nearly

depleted while only a small fraction of the VAc reacted, leaving the unreacted VAc to behave like a solvent. This resulted in a virtual solution homopolymerization of MMA at the beginning of the reaction as depicted in Figure 3. As the MMA monomer became significantly depleted, VAc began to dominate the reaction and its homopolymerization occurred. Unlike the first stage, where the autoacceleration of MMA was dampened by the solventlike effect of VAc, the VAc homopolymerization exhibited an autoacceleration attributable to an increase in viscosity. Visual observations made throughout the experiments confirmed the drastic change in viscosity. Taking the feed composition $f_{\text{MMA}0} = 0.50$ in Figure 3 as an example, it can be seen that at a conversion of roughly 60 wt %, autoacceleration began. This roughly corresponds to the monomer feed composition of 50 mol %. This behavior was further confirmed by the instantaneous copolymer composition model predictions shown in Figure 2 and the experimental cumulative composition data shown later. Similarly, for the monomer feed compositions of 20 and 40 mol % MMA, the transition

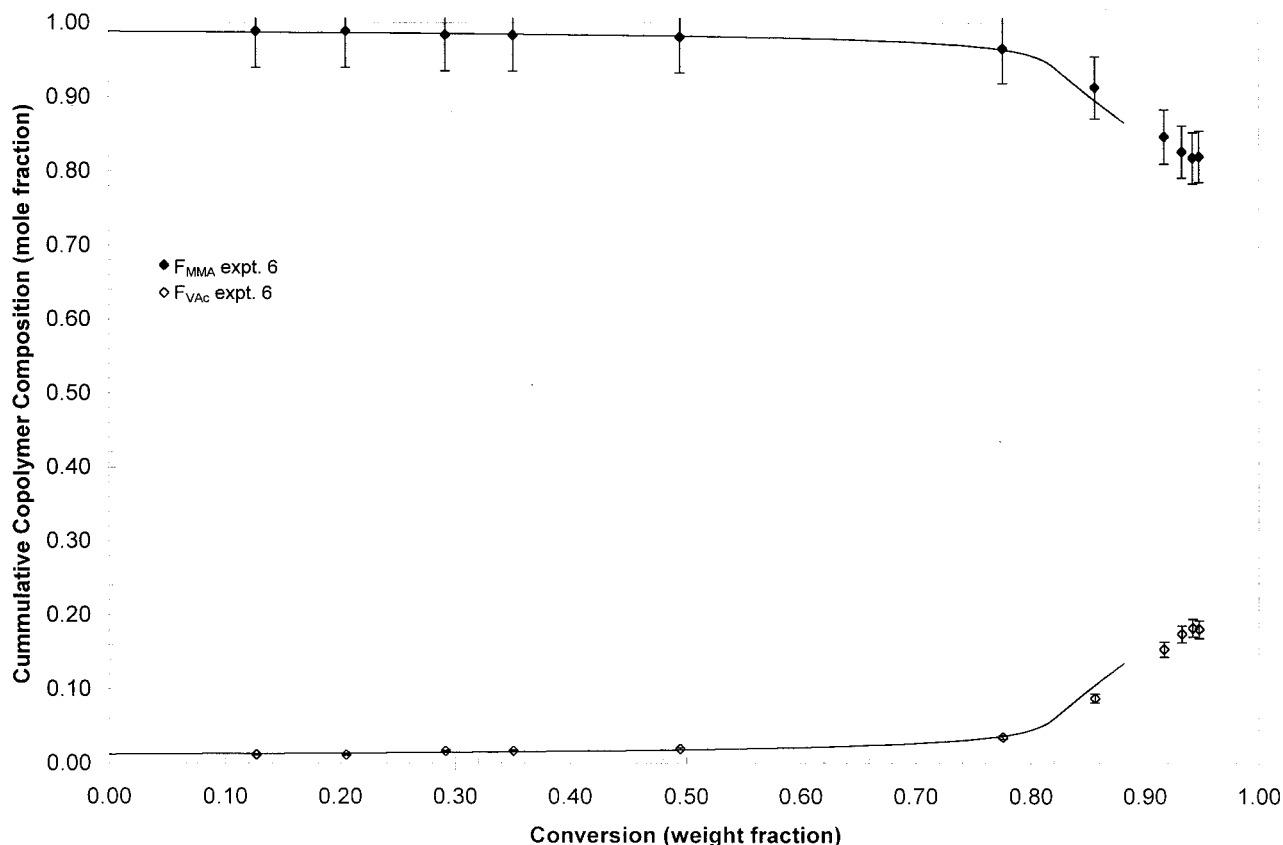


Figure 8 The cumulative copolymer composition versus the conversion ($f_{1,0} = 0.75$).

between the two reaction regimes occurred at approximately 25 and 55 wt % conversion, respectively. This indicated that for feeds more concentrated in MMA, the two-stage rate effect was delayed to higher conversions. For the feed composition of 75 mol % MMA, the two-stage rate effect was not as pronounced on conversion as in the other experiments. At such a feed composition, the system was so concentrated in MMA that the high viscosity of the reaction mixture overwhelmed the solutionlike effect of the VAc. As a result, there was no evident transition between the first part of the reaction when MMA dominated and the second part when VAc began to dominate. This transition should have occurred at about 80 wt % conversion based on the model predictions shown in Figure 2. Another distinguishing feature of the 75 mol % MMA feed experiment was that it reached a limiting conversion.

Figure 4 shows the conversion versus time results for the two feed cases (20 and 40 mol % MMA) completed at 70°C (experiments 7 and 8, Table I). These runs exhibited the same trends

with respect to the two-stage rate effect as those at 60°C. The effect occurred at approximately 30 and 50 wt % conversion for the 20 and 40 mol % MMA systems, respectively.

The trends of the effect of temperature were consistent with classical kinetics. This is shown by comparing Figures 3 and 4 for the 20 and 40 mol % MMA feed cases. These figures show that an increase in temperature greatly increased the overall rate of the reaction. At 60°C the 20 mol % MMA feed case reached full conversion in approximately 575 min while at 70°C it reached full conversion in 275 min. Therefore, an increase of 10°C in the system's temperature approximately doubled the overall rate of the reaction. A similar trend for the 40 mol % MMA feed was also observed: 100% conversion was attained in approximately 600 min at 60°C, while full conversion was reached in 275 min at 70°C.

In Figure 5 one sees the effect of adding solvent to the reaction mixture. The presence of 50 wt % toluene greatly slowed the reaction rate and dampened the two-stage rate effect. This was confirmed by comparing experiments 2 and 3 to ex-

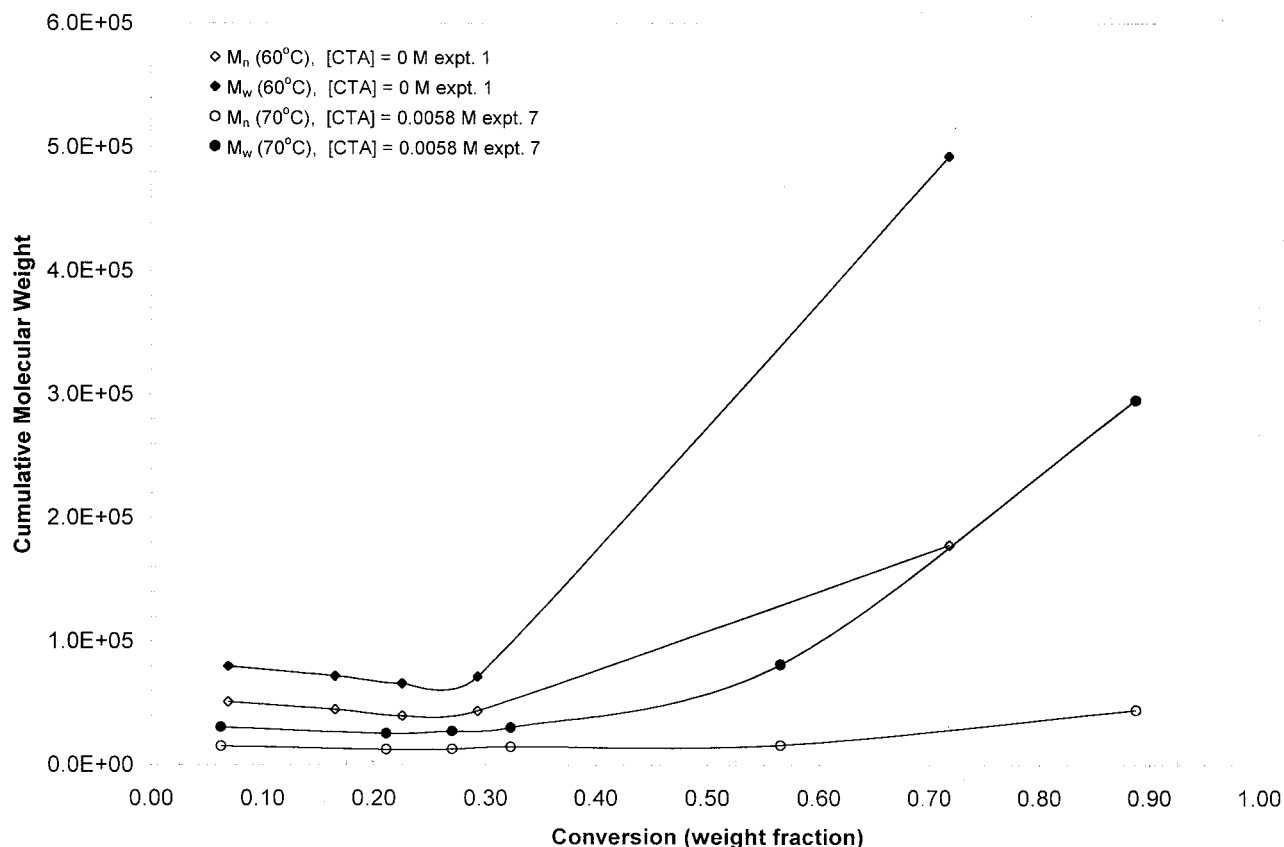


Figure 9 The cumulative number- and weight-average molecular weight versus the conversion ($f_{1,0} = 0.20$).

periment 11 in Figure 5. A similar trend was evident when comparing experiments 4 and 5 to experiment 12. The lower initiator concentration in experiment 9 also served to reduce the reaction rate according to classical kinetic theory, as seen in Figure 5. A similar trend was exhibited by experiment 10.

Cumulative Copolymer Composition

Plots of cumulative copolymer composition as a function of conversion are shown in Figures 6–8. The lines on each graph are model predictions generated using terminal model kinetics with the reactivity ratio estimates shown in Table V ($r_1 = 27.465$, $r_2 = 0.0102$).

Figure 6 presents the cumulative copolymer composition versus the conversion curves for the 20 mol % MMA feed case at 60 and 70°C. These results are typical of all of the composition data. At the beginning of the reaction, the copolymer being produced comprised mostly MMA (~88% MMA in the copolymer). However, at roughly 25

wt % conversion the amount of MMA in the copolymer drastically decreased while the amount of VAc increased. This phenomenon corroborated the existence of the two-stage rate effect discussed earlier and shown in Figure 3. One point to note is that, although the MMA polymerization dominated the beginning of the reaction, VAc was incorporated into the copolymer at all times. However, the amount of bound VAc compared to bound MMA was quite small as predicted by the low reactivity ratio for VAc. Similar to the conversion versus time plots, the copolymer composition data in Figures 6–8 indicate that as the amount of MMA in the feed was increased, the two-stage rate effect was delayed to higher conversions. However, after a certain point, increases in the MMA concentration reduced the prominence of the two-stage rate effect. This was shown in the composition data for the 75 mol % MMA feed (Fig. 8) where the two-stage rate effect was not exhibited as strongly.

Model predictions of the cumulative copolymer composition were, for the most part, reasonably

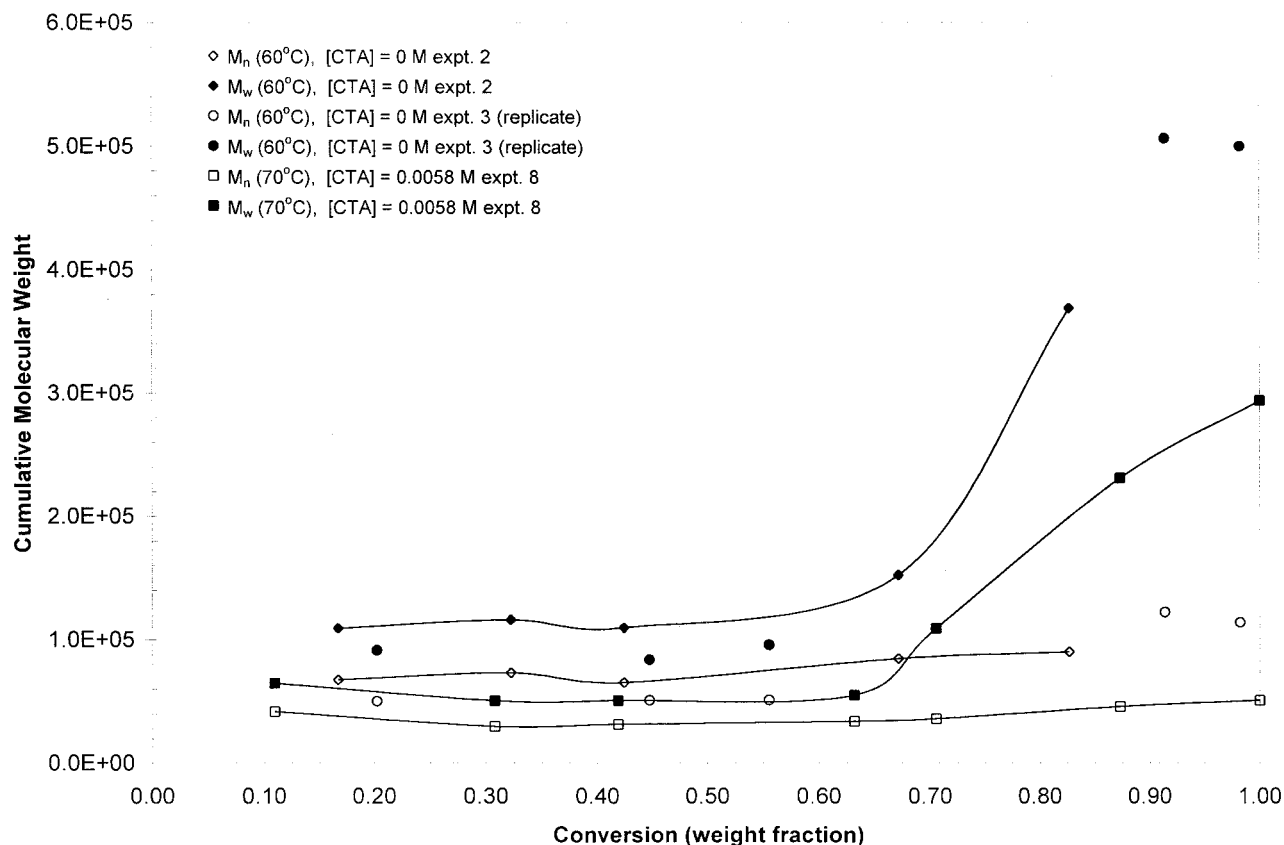


Figure 10 The cumulative number- and weight-average molecular weight versus the conversion ($f_{1,0} = 0.40$).

good. Slight differences between the model predictions and the data are apparent in Figure 6 at approximately 55% conversion. Similar differences were exhibited for the composition data from the reaction at $f_{1,0} = 0.40$. In this study the terminal model was employed to predict the experimental results. As mentioned earlier, Ma et al.¹⁸ and Brar and Charan²² showed that their *composition* data agreed with the terminal model for the MMA/VAc system and not with the penultimate unit effect model.

Figure 6 shows the data collected at both reaction temperatures. The reactivity ratios are weak functions of temperature, and thus a difference of 10°C would not be expected to influence the copolymer composition. This was supported by the data. In addition, the data from solution polymerization experiments 10 and 12 are plotted in Figure 7. No conclusive evidence of solvent effects on these data was seen. Data from the reaction at 40 mol % MMA feed were similar. Furthermore, from Figures 6 and 7 and data from the reaction at 40 mol % MMA feed,

no evidence of initiator or chain transfer effects was visible, as expected.

Cumulative Molecular Weight

Figures 9 and 10 show cumulative number- (M_n) and weight-average molecular weights (M_w) versus conversion data. The solid lines in the figures are fitted curves and do not represent model predictions. Because of the fact that some high conversion samples were insoluble, some of the plots do not contain results for samples taken toward the end of the reaction. For each bulk experiment a common trend emerged: in the beginning of the reaction the molecular weight remained fairly constant until the VAc autoacceleration occurred, at which time the high molecular weight polymers were generated. In all figures the increase in molecular weight averages corresponded to the beginning of the autoacceleration in the rate, which in turn corresponded to the feed composition, as discussed earlier for the conversion data. Although both molecular weight averages in-

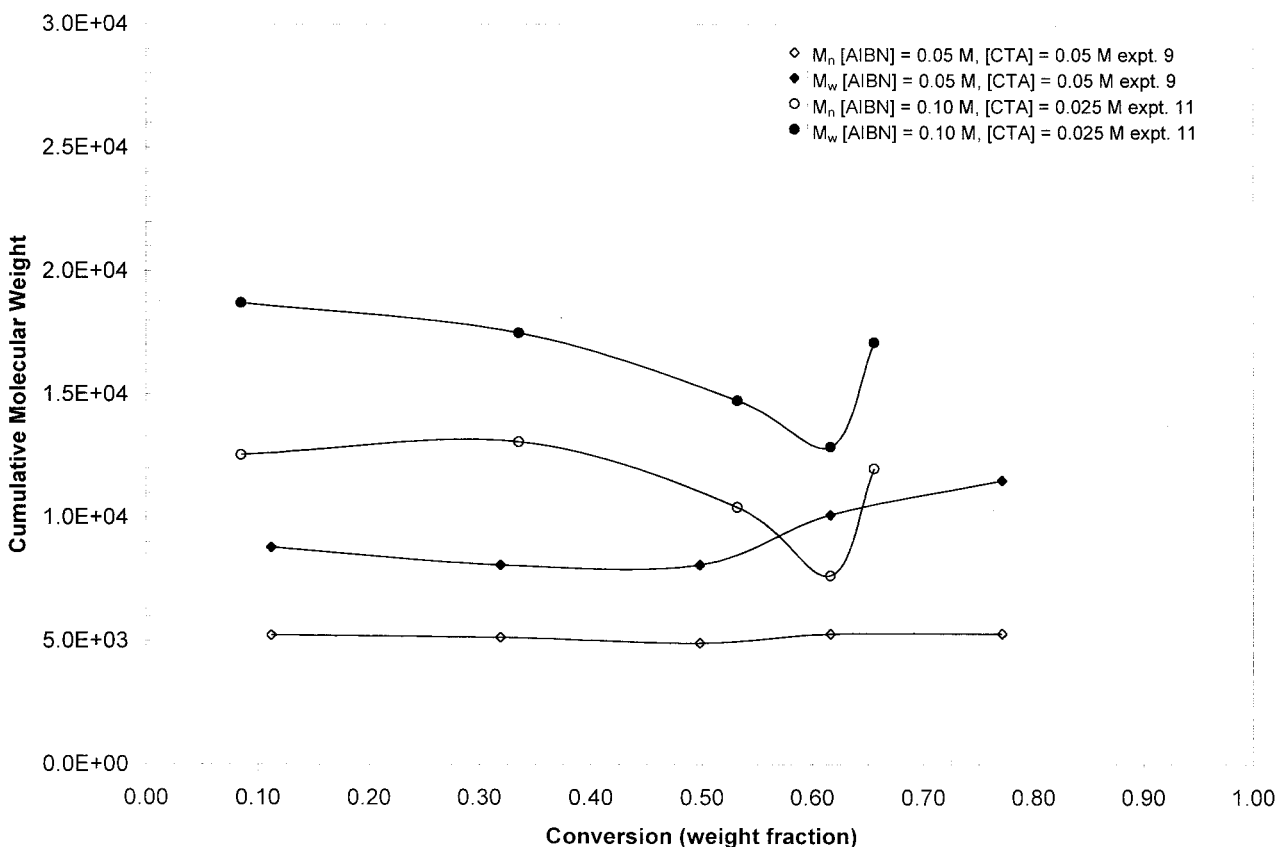


Figure 11 The cumulative number- and weight-average molecular weight versus the conversion at 60°C ([toluene] = 50 wt %, $f_{1,0} = 0.40$).

creased, the M_w showed a much larger change than the M_n when higher conversions were reached. This indicated the presence of branching reactions, such as transfer to polymer and terminal double bond reactions, common to the MMA/VAc system.²

Figures 9 and 10 illustrate the combined effect of increasing the temperature and adding CTA on the molecular weight averages for the 20 and 40 mol % MMA cases, respectively. The data showed decreases in the molecular weight averages when the temperature was increased and when CTA was added. This conformed to expected trends. It is worth noting that the high conversion samples for the runs in which no CTA was employed (i.e., runs 1–3) were difficult and often impossible to dissolve and/or filter for GPC analysis. In contrast, runs 4–12 in which CTA was added to the reaction mixture yielded highly soluble and filterable polymers even at high conversion levels.

As discussed earlier, increased amounts of MMA in the feed resulted in a faster reaction rate. This higher rate of polymerization was also

reflected in higher molecular weights. This is shown by comparing experiment 1 ($f_{1,0} = 0.20$) to experiment 2 ($f_{1,0} = 0.40$) at 60°C and experiment 7 ($f_{1,0} = 0.20$) to experiment 8 ($f_{1,0} = 0.40$) at 70°C in Figures 9 and 10. The MMA feed effect on the molecular weight was also observed for runs 4, 5, and 6.

Figure 11 provides the molecular weight averages for some of the solution polymerization runs. The figure reveals that increases in the initiator concentration resulted in higher molecular weight averages. This was expected because of the resulting increase in the reaction rate as indicated earlier in Figure 5. Experiments 10 and 12 revealed the same trends in molecular weight.

Figures 12–14 represent the molecular weight distributions (raw GPC data) for selected samples from experiments 6, 7, and 8, respectively. The progression in the molecular weight with conversion can be followed from each of these figures. It is clear from Figures 13 and 14 that high molecular shoulders appeared at higher conversions.

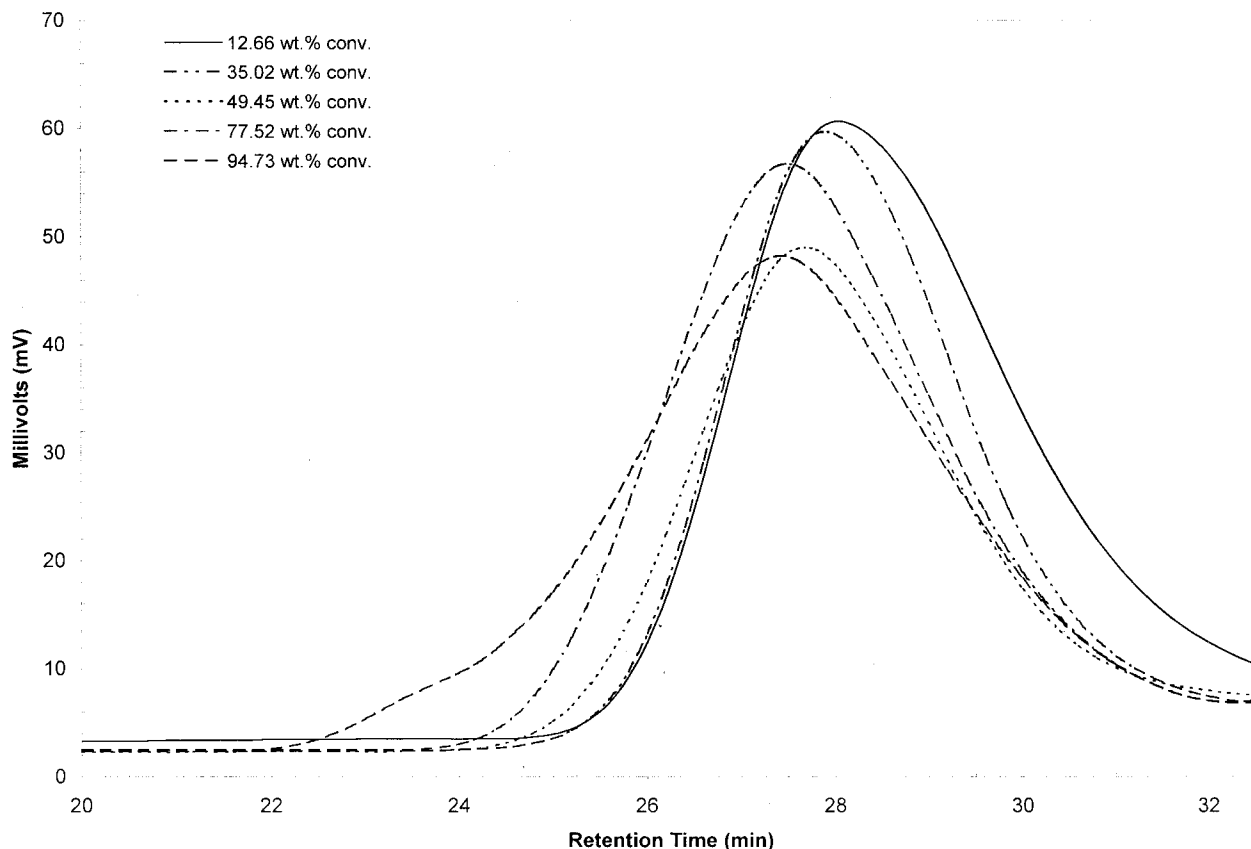


Figure 12 The molecular weight distributions ($f_{1,0} = 0.75$) at 60°C ($[AIBN] = 0.1M$, $[CTA] = 0.0058M$) for experiment 6.

This was a direct result of the autoacceleration in the rate and the branching reactions associated with VAc polymerization. Figure 12 does not reflect such a pronounced high molecular weight shoulder that was consistent with the conversion versus the time data in Figure 3 and the fact that the amount of VAc in the feed was low.

CONCLUSIONS

The results of this study coupled with the data compiled from Dubé and Penlidis² allowed a set of improved reactivity ratio estimates to be determined. When applying the EVM to the Mayo-Lewis equation, values of $r_1 = 22.760$ and $r_2 = 0.0147$ were calculated from low conversion data. Using all of the available data at both low and high conversion levels, the reactivity ratio estimates were determined using the Meyer-Lowry equation. These estimates of $r_1 = 27.465$ and $r_2 = 0.0102$ were used to predict the copol-

mer composition of the MMA/VAc system in high conversion bulk and solution experiments.

As predicted from the large difference between the two reactivity ratios, the early stage of copolymerization was dominated by MMA. Once the MMA was nearly depleted, the VAc monomer dominated the remainder of the reaction and produced an autoacceleration in the rate. This two-stage rate effect was observed to varying degrees throughout the results of 12 high conversion experiments. The results for the monomer conversion showed that increasing the feed concentration of MMA delayed the appearance of this two-stage rate effect to higher conversions. The copolymer composition results clearly showed the dominant presence of MMA in the copolymer at the beginning of the reaction followed by the dominant presence of VAc at higher conversion levels. Thus, significant composition drift was evident that demonstrated why homogeneous MMA/VAc copolymer cannot be produced in a batch reactor. Instead,

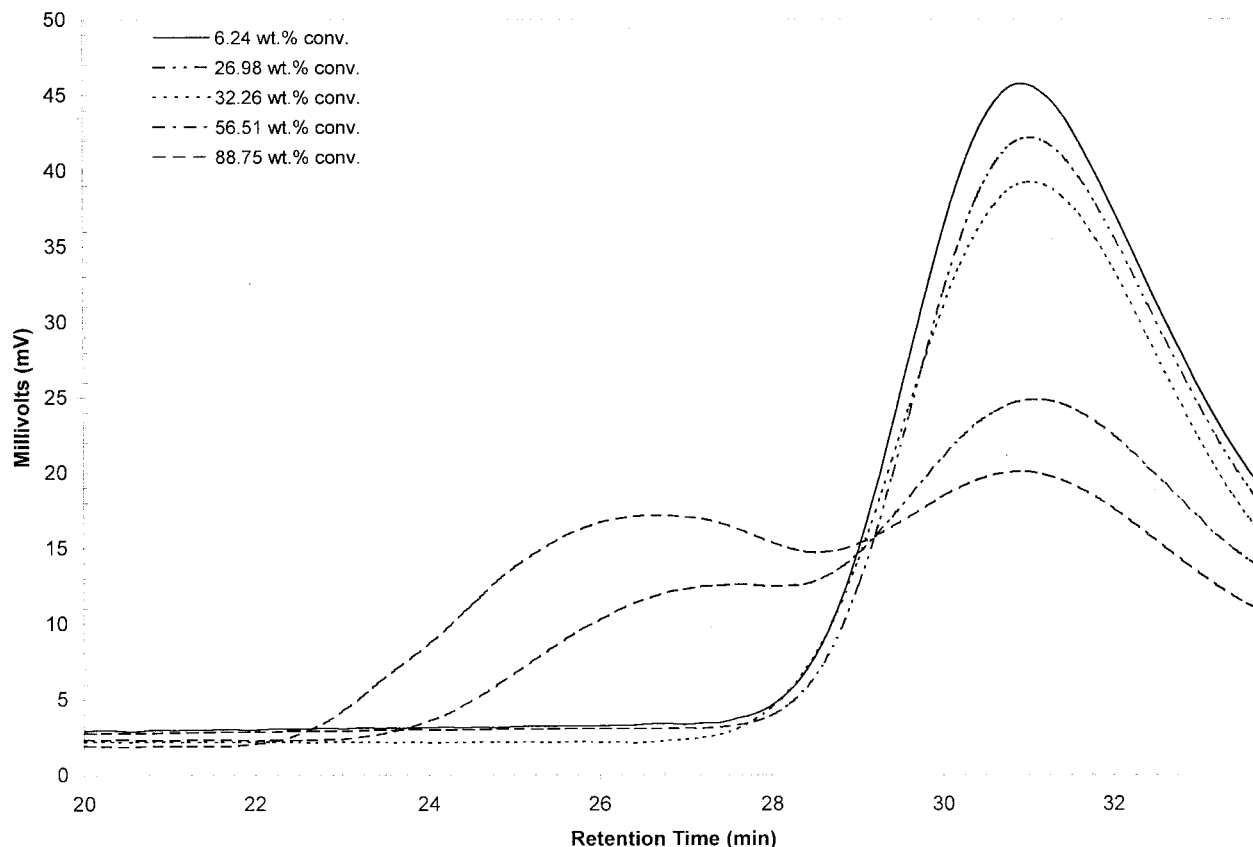


Figure 13 The molecular weight distributions ($f_{1,0} = 0.20$) at 70°C ($[AIBN] = 0.1M$, $[CTA] = 0.0058M$) for experiment 7.

semibatch reactions are needed to produce homogeneous MMA/VAc copolymers.⁸

The measurements of the cumulative number- and weight-average molecular weights displayed evidence of a two-stage rate effect. In the first phase of the reaction, the system behaved similar to a solution polymerization. This was shown by the fairly constant molecular weights that indicated that viscosity effects were not yet evident. When the system changed and began to behave as a homopolymerization, the molecular weights started to greatly increase. The molecular weight distribution data also revealed the same trends. In the first phase of the reaction, the molecular weight distributions were characterized by narrow peaks. At higher conversions, the distributions broadened and included a second peak appearing at lower retention times. This indicated that the two phases of the reaction produced polymers of extremely different molecular weights. Samples taken at high conversion levels were found to be insoluble, which was most likely due

to branching reactions that caused polymer networks.

The effects of factors such as the temperature, initiator concentration, CTA concentration, and solvent concentration conformed to expected trends. Increases in the reaction temperature and initiator concentration led to faster reaction rates and higher molecular weight averages. Because of the relatively small change in temperature, the polymer composition was not significantly changed. The addition of CTA to the reaction mixture had no appreciable effect on the rate of the reaction but significantly reduced the molecular weights of the polymers. No effect on copolymer composition was observed. Finally, the addition of solvent greatly reduced the reaction rates and lowered the molecular weights through the combined effect of increased transfer to solvent reactions and lowered reaction rates. No significant solvent effects on the copolymer composition were observed.

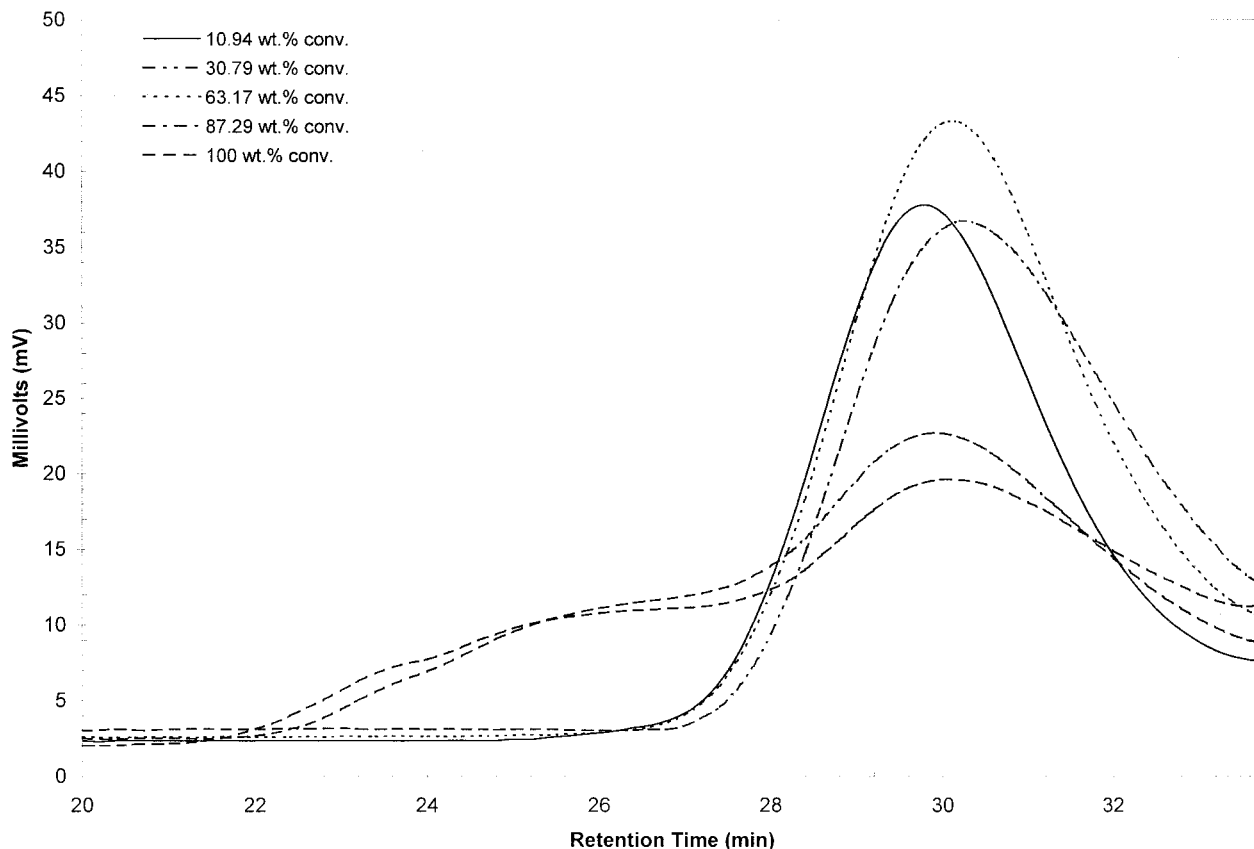


Figure 14 The molecular weight distributions ($f_{1,0} = 0.40$) at 70°C ($[\text{AIBN}] = 0.1M$, $[\text{CTA}] = 0.0058M$) for experiment 8.

These findings can now be used for the estimation of model parameters and, most importantly, for the validation and discrimination of competing kinetic models. This is the subject of our future work.

The authors wish to gratefully acknowledge financial support from the Natural Sciences and Engineering Research Council (NSERC) of Canada.

REFERENCES

1. Mayo, F. R.; Lewis, F. M. *J Am Chem Soc* 1944, 66, 1594.
2. Dubé, M. A.; Penlidis, A. *Polymer* 1995, 36, 587.
3. Brar, A. S.; Charan, S. *J Appl Polym Sci* 1994, 53, 1813.
4. Noël, L. F. J.; Van Altveer, J. L.; Timmermans, M. D. F.; German, A. L. *J Polym Sci Part A Polym Chem* 1994, 32, 2223.
5. Brar, A. S.; Charan, S. *J Appl Polym Sci* 1994, 51, 669.
6. Brar, A. S.; Charan, S. *Polymer* 1996, 37, 2451.
7. Canu, P.; Canegallo, S.; Morbidelli, M.; Storti, G. S. *J Appl Polym Sci* 1994, 54, 1899.
8. Dubé, M. A.; Soares, J. B. P.; Penlidis, A.; Hamielec, A. E. *Ind Eng Chem Res* 1997, 36, 966.
9. O'Driscoll, K. F.; Reilly, P. M. *Makromol Chem Macromol Symp* 1987, 10/11, 355.
10. Dubé, M. A.; Amin Sanayei, R.; Penlidis, A.; O'Driscoll, K. F.; Reilly, P. M. *J Polym Sci (A) Polym Chem* 1991, 29, 703.
11. Rossignoli, P. J.; Duever, T. A. *Polym React Eng J* 1995, 3, 361.
12. Polic, A. L.; Duever, T. A.; Penlidis, A. *J Polym Sci Part A Polym Chem* 1998, 36, 813.
13. Atherton, J. N.; North, A. M. *Trans Faraday Soc* 1962, 58, 2049.
14. Bevington, J. C.; Johnson, M. *Eur Polym J* 1968, 4, 669.
15. Busfield, W. K.; Low, R. B. *Eur Polym J* 1975, 11, 309.
16. Kuo, J.-F.; Chen, C.-Y. *J Appl Polym Sci* 1981, 26, 1117.
17. Bauduin, G.; Boutevin, B.; Belbachir, M.; Meghar, R. *Makromol Chem* 1990, 191, 2767.

18. Ma, Y.-D.; Won, Y.-C.; Kubo, K.; Fukuda, T. *Macromolecules* 1993, 26, 6766.
19. Burnett, G. M.; Gersmann, H. R. *J Polym Sci* 1958, 28, 655.
20. Suzuki, M.; Miyama, H.; Fujimoto, S. *J Polym Sci* 1958, 32, 445.
21. Bresler, S. E.; Kazbekov, E. N.; Shadrin, V. N. *Makromol Chem* 1974, 175, 875.
22. Brar, A. S.; Charan, S. *Eur Polym J* 1993, 29, 755.
23. Choi, K. Y.; Butala, D. N. *Polym Eng Sci* 1991, 31, 353.
24. Canegallo, S.; Canu, P.; Morbidelli, M.; Storti, G. *J Appl Polym Sci* 1994, 54, 1919.
25. Tognacci, R.; Storti, G.; Bertucco, A. *J Appl Polym Sci* 1996, 62, 2341.
26. Saldívar, E.; Ray, W. H. *AIChE J* 1997, 43, 2021.
27. Stickler, M. *Makromol Chem Macromol Symp* 1987, 10/11, 17.
28. Dubé, M. A.; Penlidis, A.; O'Driscoll, K. F. *Can J Chem Eng* 1990, 68, 974.
29. Tidwell, P. W.; Mortimer, G. A. *J Polym Sci (A)* 1965, 3, 369.
30. Armitage, P. D.; Hill, S.; Johnson, A. F.; Mykytiuk, J.; Turner, J. M. C. *Polymer* 1988, 29, 2221.
31. Zhu, S.; Hamielec, A. E. *Polymer* 1991, 32, 3021.
32. Beauchemin, R.-C.; Dubé, M. A. *Polym React Eng J* 1999, 7, 485.
33. Available at the internet site <http://www.ampolymer.com/mark-%20houwink%20parameters.htm>.
34. Brandrup, J., Immergut, E. H., Eds. *Polymer Handbook*; Wiley: New York, 1989.
35. Meyer, V. E.; Lowry, G. G. *J Polym Sci* 1965, 3, 2843.
36. McManus, N. T.; Dubé, M. A.; Penlidis, A. *Polym React Eng* 1999 J, 7, 131.